OPTICAL SPECTRA OF $Pb_{1-x}Eu_xTe$ ($0 \le x \le 1$) SOLID SOLUTION

I.I. Zasavitskiy

P.N. Lebedev Physical Institute of Russian Academy of Sciences, 53, Leninskii ave., 119991, Moscow, Russia

(Received 9 October 2008)

Optical spectra of the $Pb_{1-x}Eu_xTe$ ($0 \le x \le 1$) solid solution are analyzed. This material as high-quality epitaxial layers is at present available in labs and it is used for infrared heterolasers and Bragg mirrors. In infrared optical experiments, in addition to band-to-band transitions, the localized Eu states appear as discrete narrow or wide lines indicating the rare-earth (RE) ion interaction with crystal surrounding. The absorption and emission of the discrete lines are caused by the $4f^7(^8S_{7/2}) \leftrightarrow 4f^6(^7F_J)5dt_{2g}$ transitions. It is topical to investigate both experimentally and theoretically the energy spectrum and transition intensities in $Pb_{1-x}Eu_xTe$ in the 1 – 500 meV energy range which corresponds to the middle and far IR region. The interactions which should be taken into account are: p-d conduction band hybridization; crystal field and spin-orbit interactions for both f- and d-electrons; s-f, p-f and d-f exchange interactions.

1. Introduction

Ionic PbEuTe solid solution is a mix of the PbTe narrow gap (~ 0.2 eV) semiconductor and the EuTe wide gap (~ 2 eV) antiferromagnetic semiconductor. Varying the composition of these solid solutions it is possible to change the important material properties (band gap, refractive index) in the wide range. This opportunity was successfully used to get the effective electron and optical confinement in heterolasers [1] and in quantum-size heterostructures [2] based on the narrow gap semiconductors. In addition, now these epitaxial materials allow us to create the new, sophisticated quantum-size heterostructures and the high-reflectivity Bragg mirrors for VCSEL (vertical cavity surface emitting laser) lasers [3] and for RCED (resonant cavity enhanced detector) detectors [4] in the middle IR spectral region. It should be noted that originally it was expected that the magnetic ordering temperature of Eu chalcogenides, being below 100 K, could be raised to above 300 K by doping. This would have made them interesting for technical applications. This hope has been abandoned. However, investigation of these rare earth (RE) compounds enhanced our understanding of ferromagnetism in non-metals, and at present the solid solutions with Eu chalcogenides allow the new technological developments like the infrared VCSEL lasers and RCED detectors.

This paper analyzes the present situation with the optical transitions in the $Pb_{1-x}Eu_xTe$ ($0 \le x \le 1$) solid solution. After short information on the main properties of both Pb and Eu chalcogenides (Section 2) we will pay special attention to their optical properties. Optical properties of high-quality IV-VI semiconductor crystals are good understood and these materials are already in wide use. Basing on the literature data, the optical spectra of the Eu containing crystals and Eu monochalcogenides in the visible and ultraviolet region are discussed, and the energy diagram for Eu chalcogenides is presented (Section 3). Then the new information about optical spectra of PbEuTe solid solutions in the middle and far infrared region will be presented (Section 4). Finally, the energy scale of physical interactions in the RE optical materials will be discussed in Section 5.

2. Main properties of lead and europium chalcogenides

Mostly diamagnetic PbTe and antiferromagnetic EuTe (T_N = 9.6 K) compounds are known to crystallize in the face-centered cubic (rock salt or NaCl) crystal structure, such that one can expect (and this is confirmed by the X-ray data) that the $Pb_{1-x}Eu_xTe$ solid solution crystallizes in the lattice of the same type. The Eu^{2+} ions with a radius of 0.11 nm substitute for the Pb^{2+} cations having an ionic radius of 0.12 nm. However, the Vegard law is not satisfied, because the distribution of the Eu^{2+} ions in lattice is somewhat specific.

The properties of the lead salt binary compounds and their classical alloys have been extensively reviewed [5-7]. They are direct-gap semiconductors with the band extrema at the four equivalent L points of the Brillouin zone. Optical transitions between conduction band L_6^- and valence band L_6^+ are allowed, and tunable infrared lasers were successfully developed basing on these materials. The constant energy surfaces at the L points are prolate ellipsoids of revolution. The major axes of the ellipsoids are in the [111] directions. The conduction and valence bands at the L points are near mirror images of each other; e.g., the electron and hole effective masses are nearly equal. Effective masses are relatively small; however, nonparabolicity effect can significantly increase them. The band gap E_g and index of refraction N is a fairly strong function of alloy composition, temperature, and carrier concentration, and a typical value for PbTe at 4 K is E_g = 0.19 eV and N = 6, respectively. Transition from binary to ternary compounds can result both in the gap decrease (up to bands inversion) and in the gap increase. The strong increase of the gap takes place if the RE or alkaline earth elements form the ternary compounds.

Europium monochalcogenides are of a special interest because adding them to the lead chalcogenides we can strongly increase the band gap and change the magnetic order. There are several compounds among the RE monochalcogenides that crystallize in the face-centered cubic structure, just the same one as the lead chalcogenides possess. The four corresponding metals (Sm, Eu, Tm, Yb) tend to be in the 2^+ valence state in these compounds. Binding with the Te^{2-} ions these pairs form monochalcogenides of a semiconductor type with a large energy band gap of ~ 2 eV. However, only the europium compounds have the advantage of both the large band gap and the valence stability.

One class of divalent RE compounds, the Eu chalcogenides (EuO, EuS, EuSe, EuTe) has been investigated very thoroughly [8-11] because of their simple NaCl structure and because they are magnetic semiconductors. In the Table some properties of the Eu chalcogenides are shown: the lattice constant a_0, the Curie (or Neel) temperature $T_{C,N}$, crystal field splitting $W(e_g - t_{2g})$, exchange constants J_{nn} and J_{nnn}, absorption edge, the red shift of the absorption edge ΔW_R when temperature is lowered.

Table. Some properties of the Eu chalcogenides [9].

	a_0, (nm)	Magnetic order	$T_{C,N}$, (K)	$W(e_g - t_{2g})$, (eV)	ΔW_R, (eV)	J_{nn}, (K)	J_{nnn}, (K)	Absorption edge (eV)
EuO	0.5141	Ferro	69.3	3.1	- 0.27	- 1.212	- 0.238	1.12
EuS	0.5968	Ferro	16.6	2.2	- 0.18	- 0.472	+ 0.236	1.65
EuSe	0.6195	Antiferro or ferro	4.6	1.7	- 0.07	- 0.146	+ 0.022	1.78
EuTe	0.6598	Antiferro	9.4	1.5	+ 0.03	- 0.086	+ 0.30	2.00

Above 1 K, all the Eu chalcogenides show spontaneous magnetic order. The magnetic interaction has the same systematics as the strength of the crystal field interaction: the size of

both these interactions is proportional to the radial extension of the 5d electrons. The magnetic interaction can be described by two constants, which describe the interaction with the nearest (nn) and the next (nnn) neighbors. The J_{nnn} constant is positive (antiferromagnetic) and of about constant magnitude, whereas the J_{nn} constant is negative (ferromagnetic) and varies strongly (see Table). This integral is thought to come about by indirect cation-cation superexchange via the 5d orbitals, and it is, therefore, strongly dependent on the radial extension of these orbitals.

3. Optical spectra of Eu containing crystals and Eu monochalcogenides in the visible and ultraviolet region

Decades of scientific research on spectroscopic properties of f-shell electrons have spawned an extensive array of applications for RE activated luminescent and laser materials. These applications utilize the unique properties of the 4f electrons that have localized states and exhibit weak coupling to ligand electrons and lattice vibrations. There are also 5d, 6s, and 6p orbitals in the RE ion electronic structure. The 5d states exhibit less localized nature and stronger coupling to lattice vibrations, and since the inter-configuration $4f^n$ to $4f^{n-1}5d$ transitions of the RE ions are parity-allowed, they have intensities up to 10^4 times stronger than the strongest $4f^n$ to $4f^n$ transitions. In $4f^n$ configuration the electrons in the partially occupied 4f shell are shielded by electrons in the 5s and 5p shells from interacting with the ligands and, therefore, have little participation in chemical bond formation. As a result, the electronic transitions between the 4f states are very sharp and have atomic-like spectral characteristics.

The most impressive feature about the spectra of RE ions in ionic crystals is the sharpness of many lines in the absorption and emission spectra. It was realized that in many cases these lines can be as narrow as those commonly observed in the spectra of free atoms or free molecules. This means they sometimes have a width of $\sim 10^{-5}$ cm^{-1} or even less. For those who think of spectra of solids in terms of very broad absorption lines or bands, this feature must seem particularly attractive; it means that, in principle, it is possible to investigate interactions in a solid by optical means with a degree of accuracy similar to that usually possible with free atoms or ions.

The narrow optical lines suggest that interaction of RE ions with the crystalline environment is relatively weak. One can thus describe RE energy levels to a good degree of accuracy with a one-ion model – a very attractive approach in solid state physics.

In solid state RE spectroscopy electronic energy level structure is established primarily using the quantum theory of atomic spectroscopy, and all collective solid-state effects can be treated as a perturbation known as the crystal-field interaction.

When a 4f electron is excited into a 5d orbital that extends beyond the 5s and 5p orbitals, the spectroscopic properties of RE ions in an electronic configuration such as $4f^{n-1}5d$ are influenced more strongly by the lattice. Therefore, the electronic transitions between the $4f^n$ and $4f^{n-1}5d$ states, through absorption or emission of photons, are expected to be characteristically very different from transitions within the $4f^n$ configuration. A modification of the crystal-field theory is necessary for modeling stronger ion-lattice interactions in analysis of the energy level splitting and the excited state dynamics.

With restrictions on localized electronic interactions in a well-defined crystalline environment, the overall spectroscopic properties of a RE ion may be determined by evaluating interactions in various forms of mechanisms (see Section 5 here).

Most optical works (see, for example [9]) are concerned with the trivalent RE elements in insulators. Some RE elements, however, notably Sm, Eu, and Yb, also occur as divalent

ions in crystals. The intra-4f transitions in compounds containing divalent REs are very similar to those of the corresponding trivalent REs (where the former have an additional 4f electron, certainly). The main difference is a small compression of the energy scale brought about by smaller Coulomb and spin-orbit interactions, which are caused by the smaller effective charge of the divalent ions. For this reason the $4f^n \rightarrow 4f^{n-1}5d$ transition energies are in the ultraviolet spectral region for RE^{3+} ions and within the visible region for RE^{2+} ions.

Though no longer transparent in the rigorous sense of the word, Eu chalcogenides can be used for absorption measurements as thin films. Also, their properties have been so extensively investigated that they can serve to demonstrate the spectroscopic properties of substances, in which the spectra are dominated by the 5d electron.

The crystal field interaction for a 5d electron is larger than for a 4f electron. In comparison to it the spin-orbit interaction can also be neglected in first order. For an octahedral (cubic) coordination, the crystal field Hamiltonian for one d electron results in fivefold orbitally degenerate state which splits in a triplet and a doublet. The triplet state is a Γ_5 state and the doublet state is a Γ_3 state. More conventional, however, is the molecular orbital terminology in which the Γ_5 state is called a t_{2g} state and the Γ_3 state an e_g state. Their relative position depends on the concrete material. In the eightfold anion configuration of the fluorite lattice the e_g level has the lower energy while for the octahedral configuration of the NaCl-type lattices the order is reversed.

The ground term of the Eu^{2+} ion is $4f^7\ {}^8S_{7/2}$, the same as that of Gd^{3+}. The excited states accessible by optical spectroscopy are either $4f^7$ or $4f^65d$, both of which fall in the visible and near UV region. Absorption spectra of Eu^{2+}:SrS, Eu^{2+}:KBr and EuF_2 are dominated by two broad peaks which are shown in Fig. 1. These peaks are due to optical transitions to the 5d electron t_{2g} and e_g states. The crystal field interaction in the $4f^6$ configuration is small compared to that in the 5d state, and the energy diagram is in first order that of the free ion for $4f^6$, the ${}^6F_J$. The lowest $4f^65d$ energies should, therefore, consist of t_{2g} state (or an e_g state, depending on substance) and the ${}^6F_J$ multiplet structure is superimposed on each of them. This is indeed clearly seen in the lower absorption peak of the EuF_2 spectrum (Fig. 1). In case of EuF_2 the distances between fine structure lines vary within 0.04-0.17 eV [12].

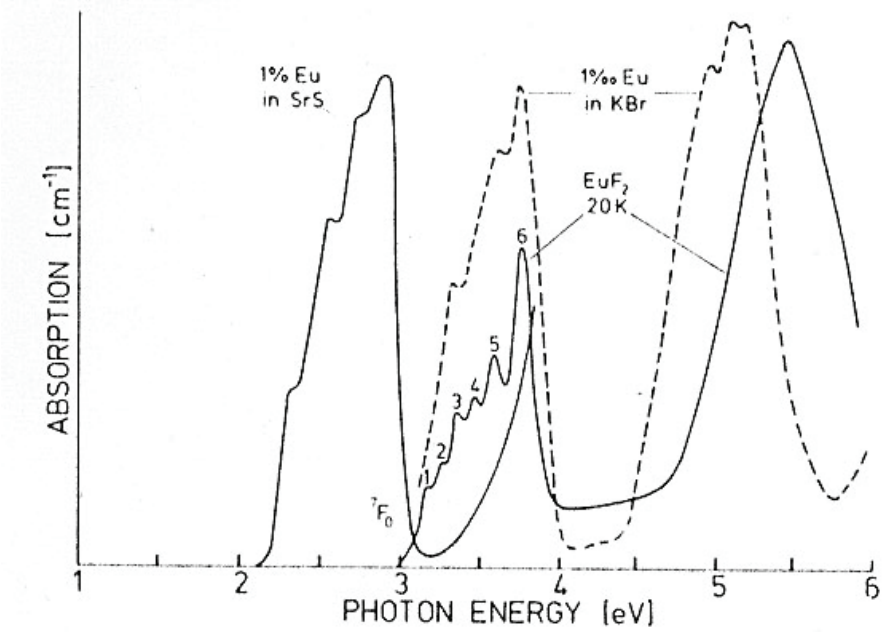

Fig. 1. Absorption spectra of Eu^{2+}:SrS, Eu^{2+}:KBr and EuF_2 [8].

Absorption spectra of the Eu chalcogenides [8, 12] are similar in their gross structure to those in Fig. 1. They show two strong absorption peaks in the region below 6 eV, which are interpreted as transitions between the $4f^7$ ground state of Eu^{2+} and $4f^6 5dt_{2g}$ and $4f^6 5de_g$ excited states. However, the fine structure on the low energy peak was not detected. The crystal field splitting $W(e_g - t_{2g})$ for each compound is shown in Table. It is important to emphasize that the center of gravity of the absorption to two 5d levels stays roughly constant through the compound series.

Taking into account this fact and other experimental data, an energy level diagram for the Eu chalcogenides was constructed [10, 13, 14] by starting from the ionic energy levels obtained by applying the appropriate Madelung correction to the free ion energy levels. The details are then filled in so as to give the best agreement with all available experimental data. Energy level diagrams obtained for the Eu chalcogenides are shown in Fig. 2. They have been brought into coincidence for the different chalcogenides by lining the position of the $4f^7$ configuration. The position of the 6s bands has been estimated and is shown by a dashed line.

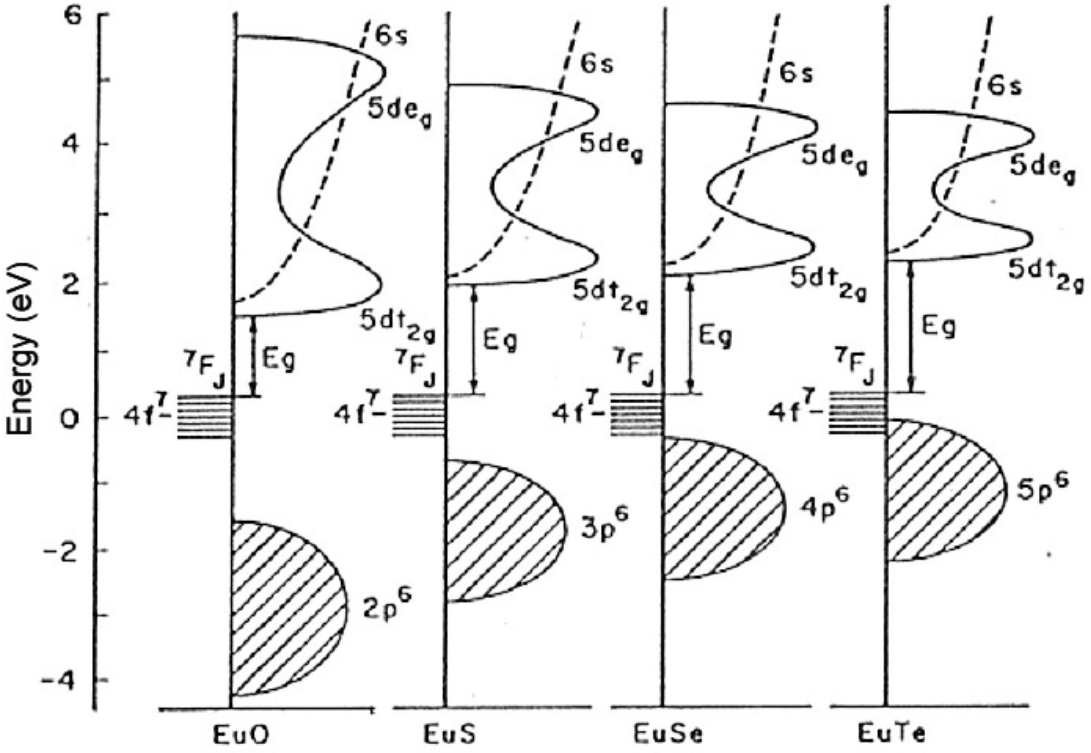

Fig. 2. Energy level diagrams for the Eu chalcogenides [10].

Luminescence investigation gives the very precise information about crystal energy spectrum and it is a powerful method to characterize the emission quantum efficiency, i.e., structure quality, composition, and uniformity. A few works were concerned with luminescence of EuTe.

A giant tunability of excitonic photoluminescence transitions was observed [15] in antiferromagnetic EuTe epilayers induced by magnetic polarons. At low temperature a narrow excitonic-like emission peak exhibiting a Stokes shift of 300 meV was detected. This peak can be tuned over a large range of 160 meV by applying magnetic field up to 5 T and it has a kink at the antiferromagnetic-paramagnetic phase transition shifting to lower temperatures with increasing magnetic field. The giant effective g-factor (~ 1000) was found. These unique

magnetic field dependences, as well as the temperature dependence of the photoluminescence transitions, result from the formation of magnetic polarons, due to d-f exchange interactions between electrons in the conduction band and localized magnetic moments.

The state of the art of the first-principle calculation of $4f^n \rightarrow 4f^{n-1}5d$ transition spectra is described in recent book [16, 17]. However, they deal with mainly visible and ultraviolet spectra.

Summarizing this paragraph, the optical properties of Eu chalcogenides in the visible and ultraviolet regions are controlled by the crystal field interaction for a 5d electron, which is one order of magnitude larger than that for a 4f electron interaction and than the spin-orbit interaction. The ^6F_J multiplet splitting was observed in absorption spectra of some Eu containing ionic crystals but not in the Eu chalcogenides.

4. Optical spectra of $Pb_{1-x}Eu_xTe$ ($0 \le x \le 1$) solid solution in the middle and far infrared region

High-quality epitaxial $Pb_xEu_{1-x}Te$ solid solutions now are available in several labs. Study of their optical properties in the middle and far infrared region is in the very beginning. There are several works concerned with optical study of this material [18-21]. Dispersion of absorption and refractive index below and above the fundamental gap was studied in $Pb_{1-x}Eu_xTe$ ($0 \le x \le 0.05$) in the frequency range 1000 – 5000 cm^{-1} at temperatures from 5 to 300 K [19]. In this work the oscillator strength, the damping parameter, and the background index of refraction were determined in detail at different compositions and temperatures.

D.L. Partin [1] has investigated the gap dependence of $Pb_{1-x}Eu_xTe$ ($0 \le x \le 0.3$) from luminescence measurements. The strong gap increase with Eu content and the nonlinear $E_g(x)$ behavior were found.

The new results were recently obtained [22] in the low temperature (10 – 100 K) photoluminescence spectra of $Pb_{1-x}Eu_xTe$ ($0 \le x \le 0.09$) solid solutions. Two types of radiative transitions were observed: an intense line corresponding to the transitions from conduction to the valence band and a series (up to 15) of narrow lines corresponding to the transitions from the hybridized conduction band to the Eu^{3+} levels.

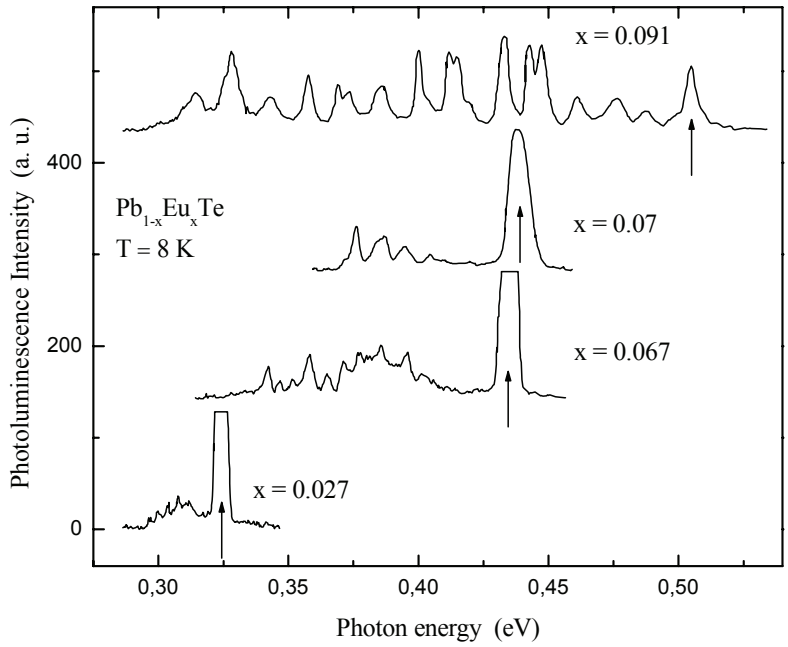

Fig. 3. Luminescence spectra of the epitaxial $Pb_{1-x}Eu_xTe$ layers of different compositions at temperature 8 K [22]. The line corresponding to the interband transitions is indicated by arrows.

We will describe these results in more detail because of their novelty. The layers were grown by MBE method and they had the thickness 1-7 μm. Excitation was accomplished by a pulsed YLF-laser at a wavelength of 1.053 μm. The excitation intensity varied within 10^4 – 10^5 W/cm^2. It was found that, in addition to the main stimulated emission line, weak narrow lines appear at lower energies when composition is increased to x ~ 0.03 (Fig. 3). As Eu content increases the intensity of the narrow lines increases and, at $x \sim 0.09$, becomes equal to the intensity of the main interband line, whose intensity noticeably decreases with the x increasing. The number of observed narrow lines also increases and reaches up to 15 at $x \sim 0.09$ at 10 K.

The halfwidth of the narrow lines is mainly determined by the resolution of grating monochromator and comprises 1 – 2 meV. The energy separation between the lines depends on the composition of the solid solution. It increases with x and changes approximately from 3 to 18 meV. The full width of the discrete spectrum including all lines is large and reaches ~ 0.2 eV at $x = 0.09$.

The observed narrow lines in the luminescence spectrum of the $Pb_{1-x}Eu_xTe$ solid solution can be naturally be associated with the RE element Eu containing an unfilled f-shell. The laser photon energy $h\nu = 1.18$ eV is appreciably higher than the energy gap E_g (L_6^- - L_6^+) = 0.19 eV in PbTe and lower than $E_g(4f^7 - 4f^6 5d^0) = 2.1$ eV in EuTe at helium temperatures. The value of E_g in EuTe corresponds to the transition between the $4f^7$ states and the excited $5dt_{2g}$ states (see Fig. 2). At relatively low Eu content ($x < 0.1$) the energy gap in $Pb_{1-x}Eu_xTe$ is determined by the transitions between the Te^{2-} p-states (L_6^+ valence band) and the hybridized L_6^- +$5d$ t_{2g} states of the conduction band. The energy scheme for the $Pb_{1-x}Eu_xTe$ solid solution and the observed radiative transitions at different x are illustrated in Fig. 4. The laser excitation induces an electronic transition to the mixed (hybridized) conduction band from the valence band and localized Eu $4f^7$ levels. After electrons are thermalized in the mixed conduction band, and their radiative recombination occurs both to the valence band (main line) and to the split ^nF_J multiplet (discrete lines).

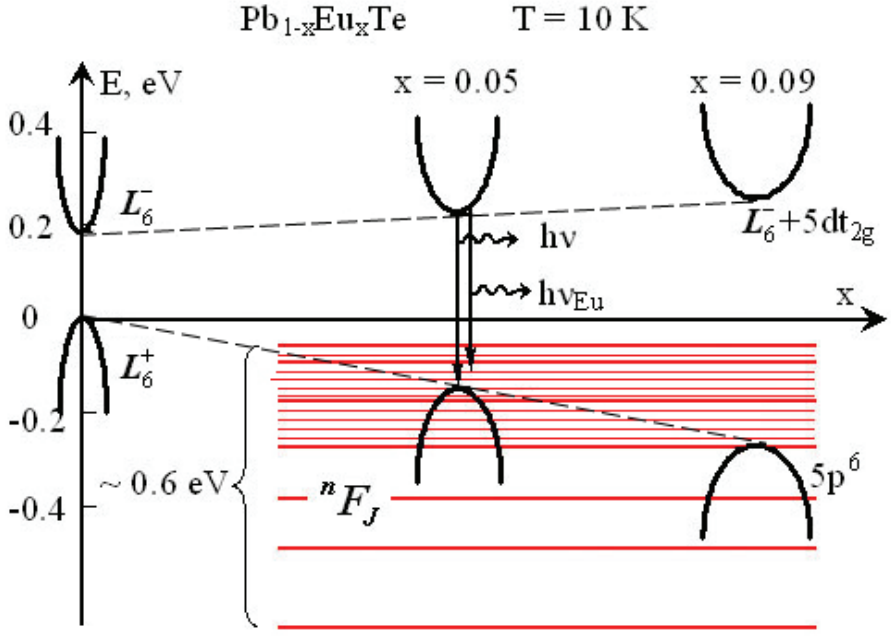

Fig. 4. Radiative transitions scheme proposed for $Pb_{1-x}Eu_xTe$ solid solution with variable compositions [22]. The dashed lines show composition movement of the L_6^- and L_6^+ band edges coming from PbTe. The notation $L_6^- + 5dt_{2g}$ band corresponds to the conduction band hybridized with the Eu d-electron excited state. The ^nF_J multiplet position and its width are taken from [9, 10, 12].

Since the wave functions of the PbTe conduction band at the *L* point in the Brillouin zone and the wavefunctions of the 4*f* levels are odd, the transitions from the 4*f* states are possible only if the even functions are admixed to the conduction band wavefunctions. Such mixing can come from the excited Eu 5*d* level, whose ground state electronic configuration can be represented as $[Xe]4f^7 5d^0 6s^2$. This level is the closest to the 4*f* level and as is known, it forms the EuTe conduction band [9, 10]. Therefore, the local replacement of the Pb 6*p* orbitals by the Eu 5*d* orbitals seems to be quite realistic.

As it is seen in Fig. 1, the absorption spectra of the Eu-doped alkaline-earth fluorides $MeF_2:Eu^{2+}$ (Me = Ca, Sr, Ba) and the EuF_2 compound consist of two broad bands generated by the $4f \rightarrow 5d$ transitions in the visible and ultraviolet spectral regions. At low temperatures (< 20 K), six peaks appear at the long-wavelength side of a band of 3 eV, with a separation between them varying from 40 to 170 meV in EuF_2 [12]. The fine structure is independent of the Eu concentration and appears due to the transitions involving the ^7F_J multiplet; i.e., these peaks correspond to the different values of the total angular momentum *J* in the $4f^6(^7F_J)$ configuration. The total width of the lower-lying band is comparable to the multiplet splitting (0.63 eV) of the Eu^{3+} ^7F_J level.

In case of PbEuTe solid solution [22], the energy scale of the fine structure is an order of magnitude lower, and the separation between the lines varies from 3 to 18 meV depending on composition.

In addition, several remarks can be done.

First, the extrapolation to x = 0 shows (see Fig. 4) that the upper edge of the ^nF_J multiplet is offset only 0.08 eV from the valence band top in PbTe, which is appreciably smaller than a value of ~ 1.2 eV derived for multiplet center from the X-ray photoelectron data [23].

Second, the theoretical estimates and experimental data suggest that the width of ^nF_J multiplet is of ~ 0.6 eV. Within the frame of this model the lower multiplet edge can be detected at compositions of x = 0.35 assuming that the oscillator strengths of the corresponding lines are large enough.

Third, the localized states can play the role of a reference for determining band discontinuities in the PbTe/PbEuTe heterojunction [24].

The first experiments were undertaken to measure the reflection and absorption in the far infrared region [25]. A series of narrow lines (at 180, 1600, and 3200 cm^{-1}) were detected at x = 0.07 and low temperatures. They can be explained by intracenter transitions. In addition, a temperature dependent line situated near 20 cm^{-1} was observed. The line is due to transverse optical phonon softening. These far infrared experimemts clearly demonstrated that there are some small (20 – 400 meV) energy interactions and splittings in the PbEuTe solid solution.

Thus, in addition to the interband transitions, radiative transitions to the Eu levels have been observed in the PbEuTe solid solution. At x = 0.09 the intensity of the discrete lines is sufficiently high and comparable with the intensity of interband line. The absorption and emission of the discrete lines are caused by the $4f^7(^8S_{7/2}) \leftrightarrow 4f^6(^7F_J)5dt_{2g}$ transitions. This finding can be used in designing IR radiation sources, in particular, in the spectral range 2 - 4 μm. For further understanding of the energy spectrum and the nature of radiative transitions, it is reasonable to calculate the Eu levels in cubic environment of the PbTe matrix and make measurements for the larger contents (up to x =1), at temperatures < 4 K, and in the presence of a magnetic field.

5. Energy scale of physical interactions in the RE optical materials

Here we would like to discuss the energy level scales of RE ions in crystals [11].

A conventional approach to solving Schrödinger equation for an *n*-electron atomic system is to use the central field approximation and Hartree-Fock method. In the central field approximation, each electron is assumed to move independently in the field of the nucleus and a central field that is made up of the spherically averaged potential fields of each of the other electrons. The quantum mechanical solution for such a central field system is the same as that for a single electron hydrogen atom. With the concept of central field approximation, the non-spherical part of the electronic interactions is treated as a perturbation to the spherically symmetric potential, so that the basis of the hydrogen atom wave functions can be used to construct wave functions for an *n*-electron atom (ion).

The primary terms of the Hamiltonian for *n*-electron ion in the absence of external fields are commonly expressed as $H = H_0 + H_C + H_{SO}$, where H_0 includes the kinetic and potential energy of the electrons in the field of the nucleus, which is purely radial and contributes to energy shifts that are the same for all the levels belonging to a configuration without affecting the energy level structure of the configuration. The term H_C represents the inter-electron Coulomb repulsion between a pair of electrons at a distance of r_{ij}, which varies for different states of the same configuration. The order of magnitude of these interactions resulting in the pure $4f^n$ configuration splitting and in the ($4f^n$ - $4f^{n-1}5d$) configuration splitting is of ~ 10^5 cm^{-1}, which is probed by UV and vacuum UV optical spectroscopy. The order of magnitude for the non-central electrostatic field correction is ~ 10^4 cm^{-1}, which is probed in the visible part of the spectrum. The interactions considered are fairly well investigated by experiment and understood by theory.

The term H_{SO} describes the spin-orbit interactions, which can be understood as magnetic dipole-dipole interactions between the spin and angular moments of the electrons. The order of magnitude of this interaction for RE ions in crystals is ~ 10^3 cm^{-1}.

Transitions within the same configuration which are strictly parity forbidden in the free ion by the Laporte rule (i.e., no electric dipole transitions between terms of equal parity!) become weakly allowed under influence of the crystalline field. Since the 4f electrons are more concentrated around the ion core than 3d electrons, and are electrostatically screened by the outer 5s, 5p electrons, the crystalline field acting on the 4f electrons is only a few 100 cm^{-1} as compared to about 10^4 cm^{-1} for the 3d electrons in iron group elements where covalency dominates. Spin-orbit interaction for 4f electrons is, on the other hand, nearly one order of magnitude larger than for 3d electrons and the Stark effect from the crystal field remains small as compared to the level separation in the multiplets. Since magnetic and solid state properties are mainly related to the lowest multiplet levels, it is sufficient to assume that in magnetic semiconductors the 4f electrons of the lanthanides conform always to the Russell-Saunders coupling scheme.

As it was mentioned above, the separation between the observed lines in PbEuTe solid solution varies from 3 to 18 meV depending on composition [22]; that is, the energy scale of the fine structure is an order of magnitude lower than in EuF_2 multiplet structure observed in the ultraviolet region. Consequently, there is some additional splitting of the IR spectra.

The intra-atomic splitting of the $^8S_{7/2}$ ground state is so small (< 10^{-5} eV) that it is observed only in the EPR measurements. The antiferromagnetic interaction with the nearest neighbors in the $Pb_{1-x}Eu_xTe$ crystals is weaker than 10^{-4} eV. As to the exchange interaction of the *f* electrons with the 6*s*, 5*p*, and 5*d* levels involved in the formation of the band states, the corresponding exchange constants for Eu^+ are equal I_{sf} = 26 meV, I_{pf} = 14 meV, and I_{df} =

98 meV and they are close to the observed splittings [26]. The spin-orbit coupling constant λ_d = 80 meV of the 5*d* level is also close to these values [26]. The Stark splitting of the RE ions in the S state is greater than ~ 10 meV. It is clear that the values of these constants in $Pb_{1-x}Eu_xTe$ crystals depend on the matrix; that is, they change with changing of Eu content.

In order to understand the nature of new spectroscopic lines observed, we should take into account the following interactions: p-d conduction band hybridization; crystal field and spin-orbit interactions for both f- and d-electrons; s-f, p-f and d-f exchange interactions.

Thus, a main conclusion coming from this analysis is that we need the measurements of optical spectra in the wide energy range (1 – 500 meV; the middle and far infrared region) where the crystal field, spin-orbit and exchange interactions take place. To compare with the experiment, the energy spectrum and oscillator strengths should be calculated for this material. Finally, a picture of physical interactions will be constructed.

References

[1] D.L. Partin, IEEE J. Quantum Electron, 24, 1716, (1988).
[2] I.I. Zasavitskii, E.A. de Andrada e Silva, E. Abramof, and P.J. McCann, Phys Rev. B, 70, 115302, (2004).
[3] W. Heiss, T. Schwarzl, J. Roither, J. Roither, G. Springholz, M. Aigle, H. Pascher, K. Biermann, and K. Reinmann, Prog. Quantum Electron, 25, 193, (2001).
[4] M. Arnold, D. Zimin, and H. Zogg, Appl. Phys. Lett., 87, 141103, (2005).
[5] Yu.I. Ravich, B.A. Efimova, and I.A. Smirnov, Semiconducting Lead Chalcogenides, Plenum Press, New York, London, 337, 1970.
[6] R. Dalven, Infrared Phys., 9, 141, (1969); and in Solid State Physics (Advances in Research and Applications), ed. by H. Ehrenreich, F. Seitz, and D. Turnball, AP, New York, 28, 179-224, 1973.
[7] T.C. Harman and I. Melngailis, Narrow-Gap Semiconductors, in Applied Solid State Science: Advances in Materials and Device Research, R. Wolfe, Ed., New York, Academic, 4, 1-94, 1974.
[8] S. Methfessel and D. C. Mattis, Magnetic Semiconductors. In Handbuch der Physik, 18/1, 389–562, Ed. by S. Flugge and H. P. J. Wijn, Springer-Verlag, Berlin, 1968.
[9] S. Hüfner, Optical Spectra of Transparent Rare Earth Compounds, AP, New York, San Francisco, London, 190, 1978.
[10] P. Wachter, Europium Chalcogenides: EuO, EuS, EuSe and EuTe. In "Handbook on the Physics and Chemistry of Rare Earth". Eds: K.A. Gschneider, Jr., LeRoy Eyring, North-Holland Publishing Company, Amsterdam, New York, Oxford, 2, 507, 1979.
[11] Spectroscopic Properties of Rare Earths in Optical Materials. Eds: G. Liu and B. Jacquier, Springer, Berlin, Heidelberg, New York, 548, 2005.
[12] M.J. Freiser, S. Methfessel, and F. Holtzberg, J. Appl. Phys., 39, 900, (1968).
[13] D.E. Eastman, F. Holtzberg, and S. Methfessel, Phys. Rev. Lett., 23, 226, (1969).
[14] J.O. Dimmock, J. Hanus, and J. Feinlleib, J. Appl. Phys., 41, 1088, (1970).
[15] W. Heiss, G. Prechtl, and G. Springholz, Physica E, 10, 419, (2001); E. Heredia, P.H. de Oliveira Rappl, P. Motisuke, A.L. Gazoto, F. Likawa, M.J.S.P. Brasil, Appl. Phys. Lett., 93, 031903, (2008).
[16] K. Ogasawara, S. Watanabe, H. Toyoshima, and M.G. Brik, In "Handbook on the Physics and Chemistry of Rare Earth", Eds: K.A. Gschneider, Jr., J.-C.G. Bunzli, and V.K. Pecharsky, North-Holland, Elsevier B.V., 37, 1, 2007.

[17] G.W. Burdick and M.F. Reid, In "Handbook on the Physics and Chemistry of Rare Earth", Eds: K.A. Gschneider, Jr., J.-C.G. Bunzli, and V.K. Pecharsky, North-Holland, Elsevier B.V., 37, 61, 2007.
[18] A. Ishida, S. Matsuura, M. Mizuno, Y. Sase, and H. Fujiyasu, J. Appl. Phys., 63, 4572, (1988).
[19] S. Yuan, H. Krenn, G. Springholz, and G. Bauer, Phys. Rev. B, 47, 7213, (1993).
[20] S. Yuan, H. Krenn, G. Springholz, Y. Ueta, G. Bauer, and P.J. McCann, Phys. Rev. B, 55, 4607, (1997).
[21] M. Aigle, H. Pascher, H. Kim, E. Tarhan, A.J. Mayur, M. Dean Sciacca, A.K. Ramdas, G. Springholz, and G. Bauer, Phys. Rev. B, 64, 035316, (2001).
[22] I.I. Zasavitskiy, A.V. Mazurin, Yu.G. Selivanov, H. Zogg, and A.V. Yurushkin, JETP Lett., 87, 498, (2008).
[23] M. Iida, T. Shimizu, H. Enomoto, and H. Ozaki, Jpn. J. Appl. Phys., 32, 4449, (1993).
[24] J.M. Langer and H. Heinrich, Phys. Rev. Lett., 55, 1414, (1985).
[25] E.V. Zhukova, B.P. Gorshunov, Yu.G. Selivanov, and I.I. Zasavitskiy, Solid State Physics, (2008), to be published.
[26] T. Kasuya, IBM J. Res. Develop., 14, 214, (1970); J. Appl. Phys., 41, 1090, (1970).